DALTON
FULL PAPER

Polybis(4-azabenzimidazolato)-iron(II) and -cobalt(II). 3-D single diamond-like framework materials which exhibit spin canting and ferromagnetic ordering at low temperatures †

Steven J. Rettig, Victor Sánchez, Alan Storr,* Robert C. Thompson * and James Trotter

Department of Chemistry, The University of British Columbia, Vancouver, B.C., V6T 1Z1, Canada. E-mail: thompson@chem.ubc.ca; storr@chem.ubc.ca

Received 31st March 2000, Accepted 26th May 2000
First published as an Advance Article on the web 21st September 2000

The direct reaction between ferrocene and an excess of molten 4-azabenzimidazole yielded amber-green crystals of polybis(4-azabenzimidazolato)iron(II), **1**. Single crystal X-ray diffraction studies revealed tetrahedrally coordinated iron ions linked by single imidazolate bridges and forming a 3-D single diamond-like (diamondoid) extended lattice. Magnetization studies show the effects of antiferromagnetic exchange above a critical temperature, T_c = 21 K, and long-range ferromagnetic ordering below this temperature, behavior that classifies **1** as a molecule-based magnet. Magnetic hysteresis studies at 4.8 K yield a coercive field, H_{coer} = 80 G and a remnant magnetization, M_{rem} = 2100 cm^3 G mol^{-1}. The isomorphous polybis(4-azabenzimidazolato)cobalt(II), **2**, has also been studied. It too is a low temperature molecule-based magnet. For **2**, T_c = 11 K and from magnetic hysteresis studies at 10 K, H_{coer} = 400 G and M_{rem} = 22 cm^3 G mol^{-1}.

Introduction

The search for and study of new molecule-based magnets, molecular materials that show spontaneous magnetization below some critical temperature, has become an area of considerable interest and activity in recent years.[1] Coordination polymers of the transition metals exhibiting such properties constitute a sub-classification of molecule-based magnets. The structural diversity of these materials and the fact that many contain ligands that are amenable to systematic derivatization raises the possibility of tailoring their properties to specific desired applications.[2]

A relatively new family of coordination polymer magnets, molecule-based, incorporates imidazolate-based ligands. It has been demonstrated that heterocyclic azolate ligands with two donor nitrogens separated by a single carbon in the ring (as in the imidazolate ion) will form single ligand bridges and extended structures. Moreover these ligands will create a bridge geometry that leads to a systematic alternation in the relative orientation of neighboring chromophores in the lattice, a situation that can produce significant spin canting and long-range ferromagnetic ordering.[3] Examples now exist of iron(II) complexes incorporating imidazolate-based ligands which, as confirmed by single crystal X-ray diffraction, have 1-D, 2-D and 3-D extended covalent lattices.[3–5] We report here the synthesis, structural characterization and magnetic properties of a new member of this family, polybis(4-azabenzimidazolato)-iron(II), **1**.

Single crystal X-ray diffraction studies reveal that in compound **1** the 4-aza nitrogen is not involved in coordination, the 4-azabenzene serving instead to create sufficient steric bulk in the imidazolate moiety to generate a unique 3-D diamond-like (diamondoid) extended lattice. The diamond-like structure in coordination polymers has attracted the attention of synthetic and materials chemists for some time now. They provide examples of 3-D "scaffolding-like materials" of potential practical importance[6,7] and are part of supramolecular chemistry and the emerging cross-disciplinary field of crystal engineering.[7,8] Since the work of Kinoshita *et al.*,[9] on bis(adiponitrile)-copper(I) nitrate, there have been a number of papers devoted to this particular molecular motif.[10] Compound **1** is the first to be reported with a totally covalent, non-interpenetrating (single) diamond-like network, exhibiting spontaneous magnetization at low temperatures.

The need to explore factors affecting characteristic properties of molecule-based magnets, such as coercivity, has recently been addressed.[11] To explore the effects of altering the d^n configuration we have synthesized and characterized polybis-(4-azabenzimidazolato)cobalt(II), **2**. Evidence indicates that **2** is isomorphous, and probably isostructural, with **1**. Although **2** also exhibits the properties of a molecule-based magnet its critical temperature, as well as coercive field and remnant magnetization at 4.8 K, are all distinctly different from those of **1**.

Experimental

Syntheses

Ferrocene, cobaltocene (both from Strem) and 4-azabenzimidazole (from Aldrich) were used as supplied. Solvents used were reagent grade and dried and distilled under an atmosphere of dry dinitrogen before use.

Syntheses

Polybis(4-azabenzimidazolato)iron(II), $[Fe(4\text{-abimid})_2]_x$, 1. Ferrocene (0.2 g, 1.07 mmol) and 4-azabenzimidazole (0.512 g, 4.3 mmol) were placed in a Carius tube which was sealed under vacuum. The tube was heated at 145 °C for 6 days. Under these conditions, the original orange solution of ferrocene in molten 4-azabenzimidazole became a mixture of a brown-red solid and an orange solution. Upon cooling to room temperature the product appeared as a crystalline brown solid embedded in the excess of non-reacted imidazole. The Carius tube was opened under a dinitrogen atmosphere. The excess of 4-azabenzimidazole was extracted with dry and oxygen-free acetonitrile and

† Based on the presentation given at Dalton Discussion No. 3, 9–11th September 2000, University of Bologna, Italy.

Electronic supplementary information (ESI) available: rotatable 3-D crystal structure diagram in CHIME format. See http://www.rsc.org/suppdata/dt/b0/b002574g/

DOI: 10.1039/b002574g

xylenes. The product was isolated as amber-green crystals suitable for single crystal X-ray analysis (Found: C, 49.4; H, 2.7; N, 28.4. Calc.: C, 49.3; H, 2.8; N, 28.7%).

Polybis(4-azabenzimidazolato)cobalt(II), $[Co(4\text{-abimid})_2]_x$, 2. Similar conditions to those employed in the preparation of compound **1** were used. Cobaltocene (0.2 g, 1.06 mmol) was utilized and the polymer isolated as described above by extraction with acetonitrile and xylenes. The product was obtained as a dark purple microcrystalline solid (Found: C, 50.1; H, 2.8; N, 28.4. Calc.: C, 48.8; H, 2.7; N, 28.5%). Repeated analysis on two different samples of **2** consistently gave good H and N results and high C. We have no explanation for the high C except to suggest there may be small amounts of solvent trapped in the sample.

Physical measurements

Infrared spectra (4000–400 cm^{-1}) were recorded at room temperature on a Bomem FTIR spectrophotometer using KBr disk samples, electronic spectra (200–3000 nm) at room temperature on Nujol mulls pressed between quartz plates using a Varian Cary 5 UV-Vis-NIR spectrophotometer. Thermal gravimetric analysis (35 to 800 °C) was done using a TA Instruments TA 2000 system with a TGA 51 unit. Magnetic properties were examined using a Quantum Design (MPMS) SQUID magnetometer. Magnetic susceptibility measurements were made at temperatures over the range 2–300 K and at applied fields of 500 and 10 000 G for both samples and at 50 and 100 G for **2**. Magnetization studies as a function of field strength (0–55 000 G) were made at several temperatures and hysteresis magnetization data obtained by oscillating the applied magnetic field between +55 000 and −55 000 G at 4.8 K for **1** and at 4.8 and 10 K for **2**. The sample holder and details regarding the use of the equipment have been described before.[12] Magnetic susceptibilities were corrected for background and for the diamagnetism of all atoms. Corrections of 140×10^{-6} cm^3 mol^{-1} were employed for $[Fe(4\text{-abimid})_2]_x$ and $[Co(4\text{-abimid})_2]_x$. All magnetic measurements were done on fine powdered samples and the data reported here are on a per mole of metal basis.

Powder diffractograms for compound **2** were recorded on a Rigaku Rotaflex RU-200BH rotating anode powder X-ray diffractometer (graphite monochromated Cu-Kα radiation). Samples were prepared by applying a hexanes slurry of the compound onto a glass plate and allowing the solvent to evaporate. The powder data were indexed employing the CRYSFIRE Suite software.[13]

X-Ray crystallographic analysis of $[Fe(4\text{-abimid})_2]_x$, 1

Crystallographic data for $[Fe(4\text{-abimid})_2]_x$, **1**, were obtained on a Rigaku/ADSC CCD diffractometer, Mo-Kα ($\lambda = 0.71069$ Å), graphite monochromator, and appear in Table 1. The data were processed[14] and corrected for Lorentz and polarization effects. The structure was solved by direct methods and expanded using Fourier techniques.[15] Hydrogen atoms were fixed in calculated positions with C–H 0.98 Å. Neutral atom scattering factors were taken from Cromer and Waber[16] and anomalous dispersion effects were included in F_{calc}.[17] Selected bond lengths and bond angles are shown in Table 2. The powder pattern for **1** was calculated, for comparison with the experimentally determined one for **2**, employing the program "PowderCell".[18]

CCDC reference number 186/2008.

See http://www.rsc.org/suppdata/dt/b0/b002574g/ for crystallographic files in .cif format.

Results and discussion

Syntheses and structures

The reaction of metallocenes with molten azoles has been utilized as an effective method for preparing divalent metal azolate polymers, often in macroscopic crystalline form.[3,5,19] In the present work the reaction between ferrocene and an excess of molten 4-azabenzimidazole has afforded a polymeric iron(II) material, $[Fe(4\text{-abimid})_2]_x$, **1**, in macroscopic crystalline form. Similarly, the reaction of cobaltocene with the same molten ligand generated the cobalt(II) material, $[Co(4\text{-abimid})_2]_x$, **2**, as a microcrystalline powder.

The compound $[Fe(4\text{-abimid})_2]_x$, **1**, was obtained in crystalline form suitable for single crystal X-ray diffraction studies. The repeat unit of **1** is shown in Fig. 1. The structure consists of iron(II) ions linked by single 4-azabenzimidazolate bridges giving a 3-D extended array (Figs. 2 and 3). The ligand binds

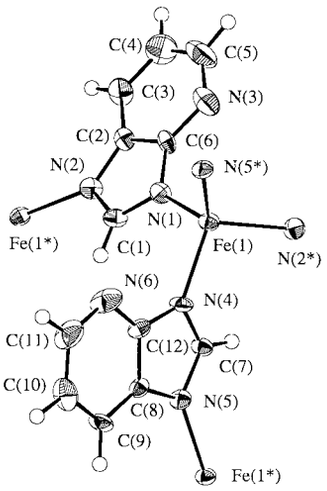

Fig. 1 View of the repeat unit of compound **1** and atom numbering scheme (33% ellipsoids).

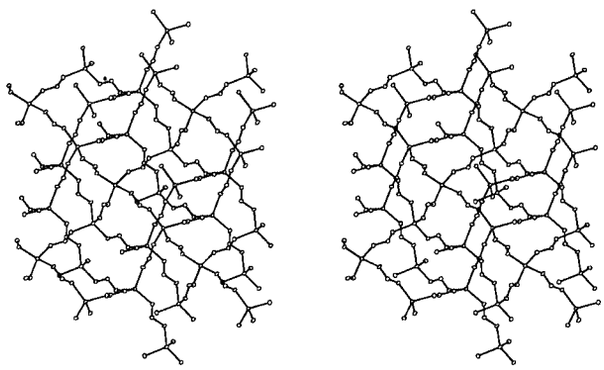

Fig. 2 Stereoscopic view of a section of the diamond-like framework of compound **1**. For clarity only the iron ions and the bridging N–C–N atoms of the imidazolate rings are shown.

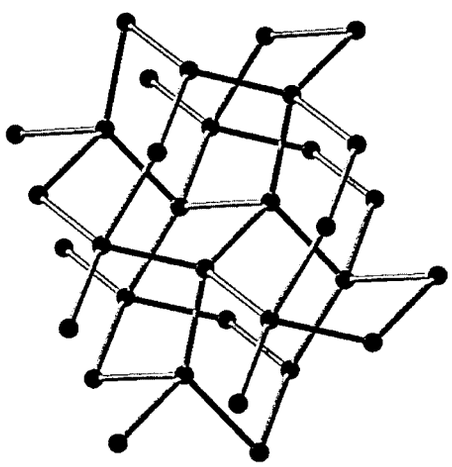

Fig. 3 Iron ion connectivity diagram for a section of compound **1**.

Table 1 Crystallographic data

Molecular formula	$C_{12}H_6FeN_6$
M	292.08
Crystal system	Orthorhombic
Space group	$P2_12_12_1$ (no. 19)
a/Å	9.655(2)
b/Å	10.3403(6)
c/Å	12.4671(7)
U/Å^3	1244.6(2)
Z	4
μ(Mo-Kα)/cm^{-1}	12.04
Total reflections	11118
Unique reflections	3233
No. with $I \geq 3\sigma(I)$	1685
R; R_w (F, $I \geq 3\sigma(I)$)	0.034; 0.024
(F^2, all data)	0.084; 0.055
R(int)	0.060
T/K	180

Table 2 Selected bond lengths (Å) and angles (°) with estimated standard deviations in parentheses *

Fe(1)–N(1)	2.030(3)	Fe(1)–N(2)[a]	2.046(3)
Fe(1)–N(4)	2.044(3)	Fe(1)–N(5)[b]	2.034(3)
N(1)–Fe(1)–N(2)[a]	110.39(11)	N(1)–Fe(1)–N(4)	102.10(11)
N(1)–Fe(1)–N(5)[b]	111.76(11)	N(2)[a]–Fe(1)–N(4)	104.31(11)
N(2)[a]–Fe(1)–N(5)[b]	109.55(11)	N(4)–Fe(1)–N(5)[b]	118.24(11)
Fe(1)–N(1)–C(1)	128.8(3)	Fe(1)–N(1)–C(6)	127.8(2)
Fe(1)[c]–N(2)–C(2)	132.6(2)	Fe(1)[c]–N(2)–C(1)	123.5(2)
Fe(1)–N(4)–C(12)	131.1(2)	Fe(1)–N(4)–C(7)	124.1(3)
Fe(1)[d]–N(5)–C(7)	127.6(2)	Fe(1)[d]–N(5)–C(8)	129.1(2)

*Superscripts refer to symmetry operations: (a) $-\frac{1}{2} + x, \frac{3}{2} - y, 1 - z$; (b) $1 - x, -\frac{1}{2} + y, \frac{3}{2} - z$; (c) $\frac{1}{2} + x, \frac{3}{2} - y, 1 - z$; (d) $1 - x, \frac{1}{2} + y, \frac{3}{2} - z$.

through the 1,3-nitrogens of the imidazolate ring. Fused rings of six distorted-tetrahedral iron centers form a unique covalently bonded diamond-like framework. Coordination of the 4-aza nitrogen is not observed. Although coordination polymers with diamond-like structures have been reported before,[9,10,20] none of them involves iron(II). Moreover, most of these materials present different degrees of interpenetration in their diamond-like arrays. Compound **1** consists of a single, non-interpenetrating, diamond-like framework. There are few examples of molecular compounds showing a single diamond-like motif. One of the most interesting studies of such structures was done by Hoskins and Robson[6a] who employed large counter ions, such as $N(CH_3)_4^+$ in $[N(CH_3)_4][Cu^IZn^{II}(CN)_4]$ and BF_4^- in $[Cu^I\{C(C_6H_4CN\text{-}4)_4\}]BF_4{\cdot}xC_6H_5NO_2$, to block the adamantane-like cavities and prevent interpenetration. The latter compound also contains molecules of nitrobenzene occupying the cavities. Another example of a single diamond-like framework was obtained in this laboratory.[21] The compound poly-bis(μ-2,5-dimethylpyrazine)copper(I) hexafluorophosphate has a cationic diamond-like lattice where the PF_6^- ions occupy positions in the lattice cavities. It should be noted that these reported single diamond-like structures have ionic lattices with counter ions occupying positions within the extended lattice, thus preventing interpenetration. To our knowledge, compound **1** is the first example of a totally covalent coordination complex having a single diamond-like framework.

Extended 3-D networks in compounds incorporating iron(II) and bridging imidazolate ligands have been observed before.[3] The 2-methylimidazolate of iron(II) has a complex 3-D network of linear channels in which ferrocene molecules, utilized in the synthesis of the material, are trapped.[3b] This contrasts with the situation seen for **1** in which there is a single non-interpenetrating diamond-like lattice with nothing trapped in the lattice cavities, a consequence, presumably, of the steric bulk of the 4-azabenzene substituent.

The X-ray powder diffractogram of $[Co(4\text{-abimid})_2]_x$, **2**, corresponds well with that calculated from the single-crystal

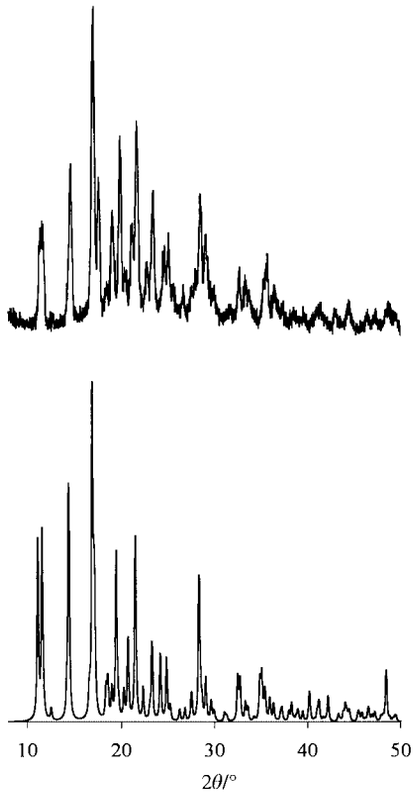

Fig. 4 X-Ray powder diffractograms of compound **2** (top, experimental) and **1** (bottom, calculated).

data of compound **1** (Fig. 4) indicating the two materials are isomorphous. Indexing the powder data[13] for **2** gave an orthorhombic unit cell with lattice parameters $a = 9.72$, $b = 10.37$ and $c = 12.45$ Å, in close agreement with those of **1** (Table 1). Further evidence that the two compounds are isostructural comes from spectroscopic studies. The electronic spectrum of **2** shows two principal absorption bands at 1125 (broad) and 580 nm with a shoulder at about 540 nm. These we assign to the $^4A_2 \longrightarrow {}^4T_1(F)$ and $\longrightarrow {}^4T_1(P)$ transitions, respectively, for tetrahedral cobalt(II).[22,23] The infrared spectra of **1** and **2** were also found to exhibit the same vibrational bands at almost identical frequencies.

The 3-D diamond-like structure seems to confer high thermal stability on polymers **1** and **2**, as shown by thermal gravimetric analysis (TGA). Compound **1** is thermally stable to 402 °C. Decomposition with continuous weight loss occurs from 402 to 476 °C with a total weight loss of 70% of the initial mass. No additional loss of mass was observed up to the maximum temperature reached of 800 °C. Compound **2** is thermally more robust than **1**, and is stable to 463 °C. This material shows a gradual weight loss amounting to 50% of the initial mass over the temperature range of 463 to 800 °C.

Magnetic properties

Magnetic susceptibilities of a powdered sample of compound **1** were measured at a field of 500 G from 2 to 300 K. Fig. 5 presents the χ *versus* T and χT *versus* T data obtained below 150 K. The value of χT decreases smoothly with temperature from the value 3.38 cm^3 K mol^{-1} at 300 K (corresponding to $\mu_{eff} = 5.20\ \mu_B$) to a low of 1.60 cm^3 K mol^{-1} just above a critical temperature, T_c, of 21 K. Below T_c, χT increases abruptly to a maximum value of 32.8 cm^3 K mol^{-1} at 14 K before decreasing again with temperature to 6.10 cm^3 K mol^{-1} at 2 K. The magnetic transition at T_c is also observed in the χ *versus* T plot (Fig. 5). The magnetic susceptibility, which increases smoothly with decreasing temperature below 300 K, shows an incipient maximum just above T_c and below T_c the magnetic suscepti-

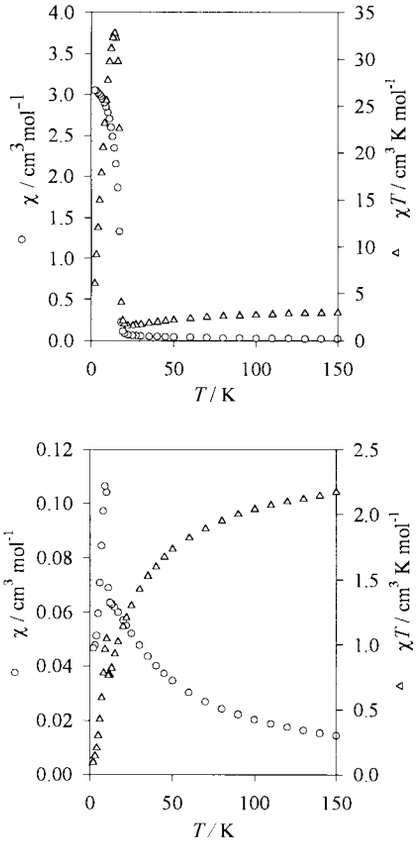

Fig. 5 Magnetic susceptibility and χT *versus* temperature plots at 500 G for compounds **1** (top) and **2** (bottom).

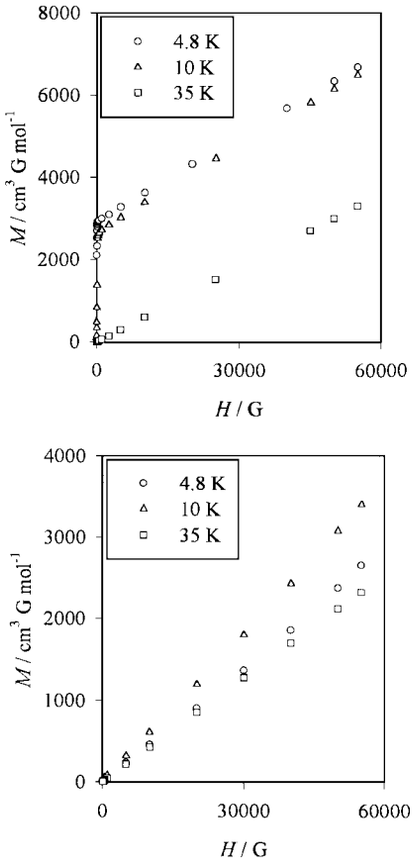

Fig. 6 Magnetization *versus* applied field plots at different temperatures for compounds **1** (top) and **2** (bottom).

bility rises abruptly as the temperature decreases before leveling off and approaching a saturation value.

This magnetic behavior exhibited by compound **1** is similar to that reported for $[Fe_3(imid)_6(Himid)_2]_x$ [3a] and $[Fe(2\text{-meimid})_2 \cdot 0.13FeCp_2]_x$.[3b] It suggests antiferromagnetic coupling in which perfect antiparallel alignment of spins on neighboring metal ions does not occur due to canting of spins. This leads to a residual spin on the metal centers as the temperature is lowered. Long-range ferromagnetic ordering of these spins below T_c generates a ferromagnetic transition. The magnetization *versus* field plots at three temperatures, shown in Fig. 6, reflect this anomalous magnetic behavior. The plot is linear at 35 K and extrapolates to zero magnetization at zero applied field while at 10 and 4.8 K (below T_c) the plots extrapolate to give a net magnetization at zero applied field. Cycling the applied field between +55 000 and −55 000 G at 4.8 K generates a hysteresis loop, the central portion of which is shown in Fig. 7. From this is obtained a remnant magnetization of 2100 cm^3 G mol^{-1} and a coercive field of 80 G.

A spin-canted structure for compound **1** is also supported by the fact that the highest magnetization reached, 6690 cm^3 G mol^{-1} (at 4.8 K and 55 000 G) is significantly smaller than the theoretical saturation value of 22 300 cm^3 G mol^{-1}.[24] Further evidence for a canted spin structure comes from the structural data of **1** which show a feature observed before in this type of system, that is a systematic alternation of the relative orientation of neighboring metal chromophores.[3,5] As a measure of this we examined the dihedral angles between the N(1)–Fe(1)–N(5) planes on adjacent, symmetry related, iron centers. On every iron center the N(1)–Fe(1)–N(5) plane forms dihedral angles of 75.4° with the corresponding planes on two of its nearest neighbors and angles of 172.5° with the corresponding planes on the other two neighbors.

In an earlier study on the related $[Fe(2\text{-meimid})_2 \cdot 0.13FeCp_2]_x$ it was observed that the anomaly at T_c is much less pronounced at the higher applied field of 10 000 G.[3b] A similar situation,

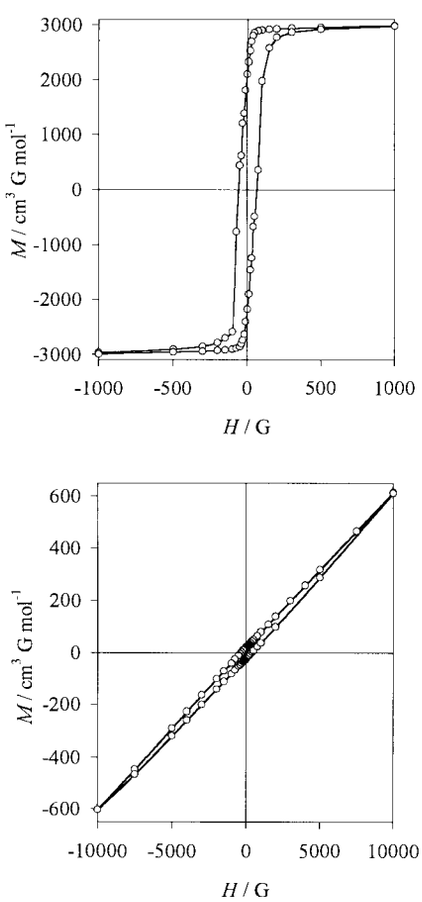

Fig. 7 Magnetic hysteresis plots at 4.8 K for compounds **1** (top) and at 10 K for **2** (bottom).

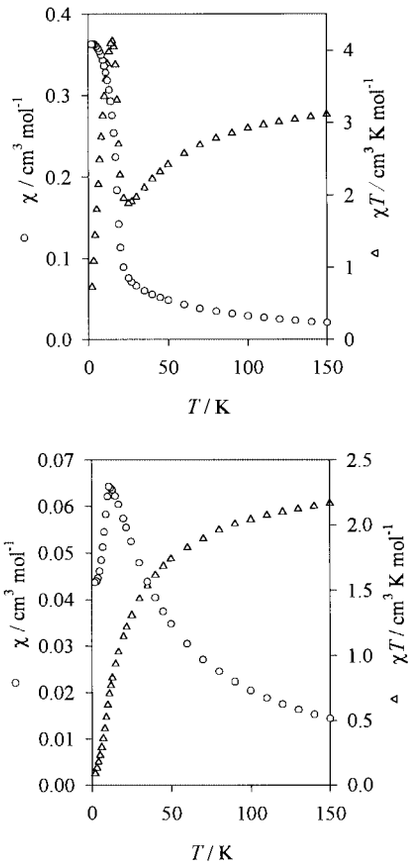

Fig. 8 Magnetic susceptibility and χT *versus* temperature plots at 10 000 G for compounds **1** (top) and **2** (bottom).

arising presumably through saturation effects, pertains to compound **1**. Plots of χT and χ *versus* T (2 to 150 K range) obtained at 10 000 G for compound **1** are shown in Fig. 8. In this case, although the maximum in χT and the saturation value of χ are both smaller than observed at an applied field of 500 G, the ferromagnetic transition is still clearly observed at 10 000 G.

The magnetic properties of compound **2** suggest that it too can be classified as a spin canted low temperature molecule-based magnet. As for **1**, χT measured at an applied field of 500 G decreases with decreasing temperature from 2.30 cm^3 K mol^{-1} at 300 K (corresponding to $\mu_{eff} = 4.29\ \mu_B$) to a critical temperature $T_c = 11$ K. Below 11 K it increases abruptly, signaling the onset of long-range ferromagnetic ordering (Fig. 5). Owing to the very small remnant magnetization present in **2** the magnetization *versus* field plots shown in Fig. 6 do not clearly display the net magnetization at zero applied field for the data obtained below T_c. The non-linearity of the plots obtained at 4.8 and 10 K is, however, evident. The highest magnetization measured for **2** was 3469 cm^3 G mol^{-1} at 10 K and 55 000 G. This is significantly lower than the theoretical saturation value of 16 766 cm^3 G mol^{-1} for a $S = 3/2$ system,[24] again consistent with spin canting providing the source of the residual spin at low temperatures.

The χ *versus* T plot for compound **2** is somewhat different from that observed for **1** (Fig. 5). For **2**, the susceptibility shows an incipient maximum just above T_c and the expected abrupt rise below T_c; however, as the temperature is lowered further, instead of showing saturation, as in **1**, χ passes through a maximum at 9 K and then decreases in value as the temperature is lowered further to 2 K (Fig. 5). This type of behavior, which suggests some loss of ferromagnetic order at the lowest temperatures, was observed previously for another cobalt(II) spin canted molecule-based magnet, polybis(formamide)bis(μ-formato)cobalt(II).[25] In this earlier study it was observed that for the formate compound this effect is not seen at lower

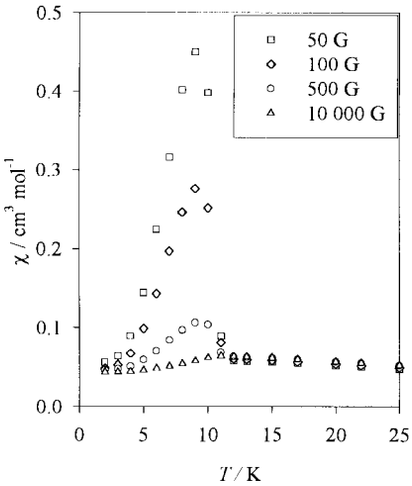

Fig. 9 Magnetic susceptibility *versus* temperature plots for compound **2** at 50, 100, 500 and 10 000 G.

applied fields. This prompted us to examine the susceptibility *versus* temperature behavior of **2** at applied fields below and above 500 G. Plots of χ *versus* T obtained at applied fields ranging from 50 to 10 000 G in the temperature range 2–25 K are shown in Fig. 9. Above T_c the susceptibilities are essentially field independent. Below T_c, at fields of 50, 100 and 500 G there is an abrupt rise in χ signaling ferromagnetic ordering. At all three of these fields the susceptibility on further cooling passes through a maximum, the magnitude of which increases with decreasing applied field strength. At the largest field studied, 10 000 G, the magnetic anomaly below T_c is not observed; the susceptibility simply passes through a single maximum at about 10 K. This is more clearly seen in Fig. 8 which also shows no clearly observable magnetic anomaly in the χT plot for **2** at 10 000 G. In Fig. 8 the susceptibility for **2** is seen to approach a constant value of ≈0.043 cm^3 mol^{-1} at the lowest temperatures, a consequence, presumably, of the spin canting. At 2 K this χ value corresponds to an effective magnetic moment of 0.83 μ_B. At the three lowest fields studied, where the anomaly indicating ferromagnetic ordering is observable, the susceptibilities decrease below 9 K and, in all cases, approach at the lowest temperature studied the same value as that recorded at 10 000 G (Fig. 9). We have no simple explanation for this decrease in susceptibility and consequent apparent loss in ferromagnetic order at low temperatures. The cause could be at the single-ion level. The $^4A_2$ electronic ground state of tetrahedral cobalt(II) is subject to zero-field splitting and if this is large enough significant changes in the population of zero-field split levels at low temperatures could affect the exchange. The significance of this factor will depend of course on the magnitude of the zero-field splitting. This may account for the fact that, although the ^5E ground state of tetrahedral iron(II) is also subject to zero-field splitting, apparent loss in ferromagnetic ordering at low temperatures is not seen for the iron analogue, **1**.

A consequence of the phenomenon just discussed for the cobalt compound, **2**, is that its hysteresis properties measured below T_c depend significantly on temperature. Measured at 10 K the hysteresis plot (central portion shown in Fig. 7) yields $M_{rem} = 22$ cm^3 G mol^{-1} and $H_{coer} = 400$ G while at 4.8 K (the temperature at which the hysteresis behaviour was measured for **1**) $M_{rem} = 6$ cm^3 G mol^{-1} and $H_{coer} = 100$ G.

Compounds **1** and **2** provide the first examples of isomorphous and presumably isostructural molecule-based magnets of two different metals. Our objective in comparing two such materials was to examine the effect on the magnetic characteristics of changing the metal. On the basis of this single study it would be dangerous to draw general conclusions and with this in mind we summarize our findings. In both **1** and **2** the metal is in a pseudo-tetrahedral geometry. In terms of single ion effects

Table 3 Magnetic parameters for some iron(II) azolate molecule-based magnets

Compound	T_c/K	H_{coer}/G	M_{rem}/cm^3 G mol^{-1}	Reference
1	21	80	2100	This work
Fe(1-Me-2-S-imid)$_2$·0.5FeCp$_2$	8	40	190	5
Fe(2-meimid)$_2$·0.13FeCp$_2$	27	5000	200	3(*b*)
Fe$_3$(imid)$_6$(Himid)$_2$	17	200	2500	3(*a*)
Fe(4-imidac)$_2$·2CH$_3$OH	15	6200	1200	4
Fe(biimid)	25	2000	950	27

Abbreviations: T_c = critical temperature, H_{coer} = coercive field, M_{rem} = remnant magnetization, imid = imidazolate, 4-imidac = 4-imidazoleacetate, biimid = biimidazolate.

there is no first-order orbital contribution to the magnetic moment in either case[26] and the primary difference lies in the spin contributions, $S = 2$ for **1** and $S = 3/2$ for **2**. This may, partly at least, contribute to the smaller remnant magnetization observed for **2** (6 cm^3 G mol^{-1} at 4.8 K and 22 cm^3 G mol^{-1} at 10 K) compared to that for **1** (2100 cm^3 G mol^{-1} at 4.8 K). It seems likely, however, that the degree of spin canting would be much more important in this regard. The coercive fields are not as different in the two materials. This quantity, defined as the applied field required to return the magnetization of the sample to zero, is 80 G (at 4.8 K) for **1** and 100 G at 4.8 K (400 G at 10 K) for **2**. In terms of hysteresis behavior another characteristic property is the range of applied fields over which the magnetization of the sample is dependent on the history of the field sweep (increasing or decreasing). In this regard the samples are quite different. For **1** this field range is approximately ±1000 G at 4.8 K while for **2** it is about ±10 000 G at 10 K. At 4.8 K the magnetization of **2** is dependent on the history of the field sweep over the entire range of fields studied. Finally we note that the magnetic anomaly at T_c is observable at higher applied fields for **1** than for **2** and that the apparent loss in ferromagnetic order at low temperatures and all fields exhibited by **2** is not observed for **1**. To establish the generality of such findings we are investigating other isomorphous pairs of iron and cobalt compounds.

Table 3 shows the magnetic parameters for six iron(II) azolate polymers, including **1**, which exhibit canted spin antiferromagnetism and low temperature ferromagnetic ordering. All except the biimidazolate compound[27] have been structurally characterized by single crystal X-ray crystallography. The three dimensional structures are all different, a factor which makes meaningful comparison of parameters difficult. The compounds Fe$_3$(imid)$_6$(Himid)$_2$,[3a] Fe(2-meimid)$_2$·0.13FeCp$_2$[3b] and **1** all have covalent bonding interactions connecting the paramagnetic centers in three dimensions, Fe(4-imidac)$_2$·2CH$_3$OH[4] has covalent bonding interactions connecting the metal centers in two dimensions and hydrogen-bonding interactions connecting the sheets and Fe(1-Me-2-S-imid)$_2$·0.5FeCp$_2$[5] has covalent interactions generating a one dimensional structure with only van der Waals interactions connecting the chains. This comparison points to the fact that the presence of spin canting and long-range ferromagnetic order does not seem to require a particular molecular motif or covalent bonding dimensionality. We note, however, as Kahn[1a] has pointed out, the antisymmetric interaction[28,29] is at the origin of spin canting in extended lattices of very low symmetry. This is possibly the case here where single-bridging imidazolate ligands generate low symmetry M–L–M exchange pathways.

Acknowledgements

Funding for the project was provided by the Natural Sciences and Engineering Research Council of Canada. P. Borda of this department is thanked for the C, H and N analyses and B. Patrick for assistance with interpretation of crystallographic data.

References

1 (*a*) O. Kahn, *Molecular Magnetism*, VCH, New York, 1993; (*b*) M. M. Turnbull, T. Sugimoto and L. K. Thompson, *ACS Symp. Ser*., 1996, **644**; (*c*) D. Gatteschi, *Adv. Mater.*, 1994, **6**, 635; (*d*) K. Itoh, J. S. Miller and T. Takui, *Mol. Cryst. Liq. Cryst.*, 1997, **305/306**; (*e*) O. Kahn, *Adv. Inorg. Chem.*, 1995, **43**, 179.
2 J. S. Miller and A. J. Epstein, *Angew. Chem.*, *Int. Ed. Engl.*, 1994, **33**, 385; E. Coronado, P. Delhaès, D. Gatteschi and J. S. Miller (Editors), *Molecular Magnetism: From Molecular Assemblies to the Devices*, NATO ASI Series C, Kluwer Academic, Dordrecht, 1996, vol. 321.
3 S. J. Rettig, A. Storr, D. A. Summers, R. C. Thompson and J. Trotter, (*a*) *J Am. Chem. Soc.*, 1997, **119**, 8675; (*b*) *Can. J. Chem.*, 1999, **77**, 425.
4 M. A. Martinez-Lorente, V. Petrouleas, R. Poinsot, J. P. Tuchagues, J. M. Savariault and M. Drillon, *Inorg. Chem.*, 1991, **30**, 3587.
5 S. J. Rettig, V. Sánchez, A. Storr, R. C. Thompson and J. Trotter, *Inorg. Chem.*, 1999, **38**, 5920.
6 (*a*) B. F. Hoskins and R. Robson, *J. Am. Chem. Soc.*, 1990, **112**, 1546; (*b*) L. R. MacGillivray, S. Subramanian and M. J. Zaworotko, *J. Chem. Soc.*, *Chem. Commun.*, 1994, 1325.
7 M. Ward, *Chem. Br.*, 1998, September, 52.
8 M. Munakata, L. P. Wu and T. Kuroda-Sowa, *Adv. Inorg. Chem.*, 1999, **46**, 173.
9 Y. Kinoshita, I. Matsubara, T. Higuchi and Y. Saito, *Bull. Chem. Soc. Jpn.*, 1959, **34**, 1221.
10 O. Ermer, *Adv. Mater.*, 1991, **3**, 608; B. F. Abrahams, M. J. Hardie, B. F. Hoskins, R. Robson and G. A. Williams, *J. Am. Chem. Soc.*, 1992, **114**, 10641; O. M. Yaghi, D. A. Richardson, G. Li, E. Davis and T. L. Groy, *Mater. Res. Soc. Symp. Proc.*, *371 (Adv. in Porous Materials)*, 1995, **15**; T. Vossmeyer, G. Reck, L. Katsikas, E. T. K. Haupt, B. Schulz and H. Weller, *Science*, 1995, **267**, 1476; T. Kuroda-Sowa, M. Yamamoto, M. Munakata, M. Seto and M. Maekawa, *Chem. Lett.*, 1996, 349; T. Kuroda-Sowa, T. Horino, M. Yamamoto, Y. Ohno, M. Maekawa and M. Munakata, *Inorg. Chem.*, 1997, **36**, 6382; S. Lopez, M. Kahraman, M. Harmata and S. W. Keller, *Inorg. Chem.*, 1997, **36**, 6138; S. M. Stalder and A. P. Wilkinson, *Chem. Mater.*, 1997, **9**, 2168; E. Siebel, A. M. A. Ibrahim and R. D. Fischer, *Inorg. Chem.*, 1999, **38**, 2530; W. Choe, Y.-H. Kiang, Z. Xu and S. Lee, *Chem. Mater.*, 1999, **11**, 1776.
11 M. G. F. Vaz, L. M. M. Pinheiro, H. O. Stumpf, A. F. C. Alcântara, S. Golhen, L. Ouahab, O. Cador, C. Mathonière and O. Kahn, *Chem. Eur. J.*, 1999, **5**, 1486.
12 M. K. Ehlert, S. J. Rettig, A. Storr, R. C. Thompson and J. Trotter, *Can. J. Chem.*, 1989, **67**, 1970.
13 R. Shirley, *The CRYSFIRE System for Automatic Powder Indexing: User's Manual*, The Lattice Press, Guildford, 1999; J. W. Visser, *J. Appl. Crystallogr.*, 1969, **2**, 89.
14 TEXSAN, Crystal Structure Analysis Package, Molecular Structure Corporation, Houston, TX, 1985 and 1992.
15 SIR 92, A. Altomare, M. Cascarano, C. Giacovazzo and A. Guagliardi, *J. Appl. Crystallogr.*, 1993, **26**, 343; DIRDIF 94, P. T. Beurskens, G. Admiraal, G. Beurskens, W. P. Bosman, R. de Gelder, R. Israel and J. M. M. Smits, The DIRDIF 94 program system, Technical Report of the Crystallography Laboratory, University of Nijmegen, 1994.
16 D. T. Cromer and J. T. Waber, *International Tables for X-Ray Crystallography*, The Kynoch Press, Birmingham, 1974, vol. IV, Table 2.2 A.
17 J. A. Ibers and W. C. Hamilton, *Acta Crystallogr.*, 1964, **17**, 781.
18 PowderCell, version 2.3, W. Krauss and G. Nolze, Federal Institute for Materials Research and Testing (BAM), Berlin, 1998.
19 D. A. Summers, Ph.D. Thesis, University of British Columbia, 1997.

20 J. L. Manson, W. E. Buschmann and J. S. Miller, *Angew. Chem.*, *Int. Ed.*, 1998, **37**, 783.
21 T. Otieno, S. J. Rettig, R. C. Thompson and J. Trotter, *Inorg. Chem.*, 1993, **32**, 1607.
22 A. M. Vecchio-Sadus, *Transition Met. Chem.*, 1995, **20**, 46.
23 M. K. Ehlert, A. Storr and R. C. Thompson, *Can. J. Chem.*, 1993, **71**, 1412.
24 R. L. Carlin, *Magnetochemistry*, Springer-Verlag, Berlin, 1986, pp. 7–9.
25 S. J. Rettig, R. C. Thompson, J. Trotter and S. Xia, *Inorg. Chem.*, 1999, **38**, 1360.
26 B. N. Figgis and M. A. Hitchman, *Ligand Field Theory and Its Applications*, Wiley-VCH, New York, 2000.
27 M. A. Martinez-Lorente, F. Dahan, Y. Sanakis, V. Petrouleas, A. Bousseksou and J. P. Tuchagues, *Inorg. Chem.*, 1995, **34**, 5346.
28 I. Dzialoshinsky, *J. Phys. Chem. Solids*, 1958, **4**, 241.
29 T. Moryia, *Phys. Rev.*, 1960, **120**, 91.